Article QR

Title:	**Nuclei Spotting for Computational Pathology in Microscopic Images**
Author (s):	Abdul Basit Syed[1], Samabia Tehsin[2], Sumaira Kausar[1]
Affiliation (s):	[1]Department of Computer Science, Bahria University Islamabad, Pakistan [2]Department of Computer Science, Bahria University, Karachi Campus, Pakistan
DOI:	https://doi.org/10.32350.umt-air.21.05
History:	Received: April 19, 2022, Revised: May 27, 2022, Accepted: June 9 19, 2022
Citation:	A. B. Syed, S. Tehsin, and S. Kausar, "Nuclei spotting for computational pathology in microscopic images," *UMT Artif. Intell. Rev.,* vol. 2, no. 1, pp. 00–00, 2022, doi: https://doi.org/10.32350.umt-air.21.05
Copyright:	© The Authors
Licensing:	This article is open access and is distributed under the terms of Creative Commons Attribution 4.0 International License
Conflict of Interest:	Author(s) declared no conflict of interest

Nuclei Spotting for Computational Pathology in Microscopic Images

Samabia Tehsin[1*], Sumaira Kausar[1] and Syed Abdul Basit[2]

[1]Department of Computer Science, Bahria University Islamabad, Pakistan
[2]Department of Computer Science, Bahria University Karachi Campus, Pakistan

Abstract-**Nuclei spotting has been given a paramount importance in diagnosing and monitoring many medical conditions. It also helps the pharmacists to develop and discover new formulas of drugs/remedy by observing the effects of medicines on the patients. Nuclei spotting becomes a challenging task due to the natural variation in the appearance as well as the variation of image capturing devices. Besides, variation in the lightening conditions also pose extra challenges in the process of detection and segmentation of nuclei. In the current study, we employed a modified U-Net (mU-Net), a deep learning-based approach, for nuclei detection and segmentation. The results showed the supremacy of the proposed method. Intersection over Union (IOU) of 0.78 was achieved on BBBC038v1 dataset.**

Index Terms-**Deep learning, digital pathology, nuclei detection, U-Net**

I.Introduction

The current study claimed that people from all over the world get infected with various types of diseases including cancer, chronical diseases, brain and heart issues, diabetes and Alzheimer's. The drugs for Alzheimer's and Parkinson's diseases are too expensive and takes plenty of time to be at one's disposal in the market. Therefore, many companies working on the research and development of drugs for Parkinson's and Alzheimer's diseases have stopped to develop new medicines. Recent studies indicated that development of a new medicine, from target identification through approval for marketing, takes over 12 years and often much longer to discover a new drug [1]. The assessment process of most diseases has become expeditious due to the advancement in the field of medical imaging. The methodologies of automatic nucleus classification, nucleus, and detection algorithms have been

---
[*] Corresponding author: stehseen.buic@bahria.edu.pk

adopted for the fast diagnosis and cure of many critical diseases, that is, cancer. The starting point is to identify cell nuclei. The analysis contains 30 trillion cells. These cells contain nuclei which are full of DNA of human body. The accurate identification of the cell function helps the researchers to examine how cells react together to discover different cures and treatments. Moreover, the researchers become capable to understand the biological processes after such an identification at the cell level. This solution provides with the faster treatment of patients and better outcomes in terms of medicines discovery. Therefore, the field of microscopy imaging and computational pathology play a cardinal role in the diagnosis of different diseases. Furthermore, these images contain a lot of information for CAD. Therefore, the throughput/output rate for the analysis of images can become very high. Currently, the computational-pathology has become spearhead and renowned in the research of medical imaging. Also, it has become serviceable for the patients as well as for the pathologists. Thus, the computational-pathology has achieved significant attention from the researchers and the clinical practice community [2]. As the computational techniques give efficient outcome and accelerates the process of image analysis as compared to the traditional and manual systems for clinicians and researchers. In manual image analysis, the computational-pathology and the microscopic-imaging are very challenging procedures to deal with. Therefore, it leads to large inter-observer variations. Besides, CAD characterizes the diseases very accurately and minimizes the bias in a significant way. Moreover, the computational pathology provides measurements of pathological images which can be reproduced for clinical follow-ups. The current study aims to personalize treatment process and drug's discovery, which is ultimately helpful for patients. The computerized approach gives fast image analysis as compared to the time consuming manual assessment, which releases the researchers from repeated and boring routine efforts. In order to handle the huge amount of dataset, grid computing and computationally scalable algorithms provide high throughput/output for analyzing pathology images. Whereas, the nuclei detection and segmentation is the critical prerequisite of CAD and it is also considered as a basis of automated image analysis. Furthermore, it provides analysis for calculating size, shape,

morphology, and texture of cells. However, a robust and accurate segmentation of nuclei is very difficult. In histopathology and microscopy, images contain background clutter, noise, blurred-region during image acquisition, and poor contrast. Moreover, there are variations in size, shape, and intracellular intensity of nuclei. In the similar manner, nuclei are very close to each other and often overlap with one another. Figure 1, pictorially explains the detection and segmentation of Nuclei. Many researches have been conducted for the sake of automatic nucleus detection and segmentation, which is eventually aimed to improve detection accuracy.

The proposed research focuses on the improved nuclei segmentation with cluttered background, varying acquisition devices, and natural variation of nucleus structure. Besides, the presented work performs modification in U-Net deep learning based architecture. Also, the results based on the BBBC038v1 dataset [4] validates the primacy/priority of the proposed methodology. The proposed research significantly improves the segmentation accuracy of the state of art work.

II. Related Work

The literature of this study showed that there are several different state-of-the-art methods for detecting and localizing the nuclei. Lin et al. [5] and Bhattacharjee et al. [6] perform very well on the detection process, but do not control output masks. Lu et. al [7] demonstrates the effectiveness of combining the object proposals and the edge detection together. As they utilize the unsupervised training session, so we are unsure if it would have been competitive to implement in this research or not. In this case, others have focused on detecting tumors and have been classifying them, while this research does not focus on classification.

The feature-based representation utilized in Khoshdeli et. al [8] shows promise as a preprocessing method, but the most difficult problem in constructing good masks for the data in this research is separating the overlapping nuclei. Therefore, we are unsure if this feature-based representation would help with this issue or not. Since, it is mainly a tool for accentuating nuclei from the background. In Xie *et al.* [9] focus on the cell detection by outputting a cell centroid but not a mask. Thus, they would require adaption in

procedure, if they were to be used for different data.

However, the researchers discovered that this problem is an instance segmentation problem which is a complex issue and one of the most challenging computer vision tasks, which can further perform instance segmentation by detecting the objects and predicting the pixel-level instances on objects. There are several state-of-the-art methods for instance segmentation in medical imaging. Few methods focused on the overlapping of cells. Dynamic priors and fuse deep CNNs are utilized for the above mentioned problem [5, 8].
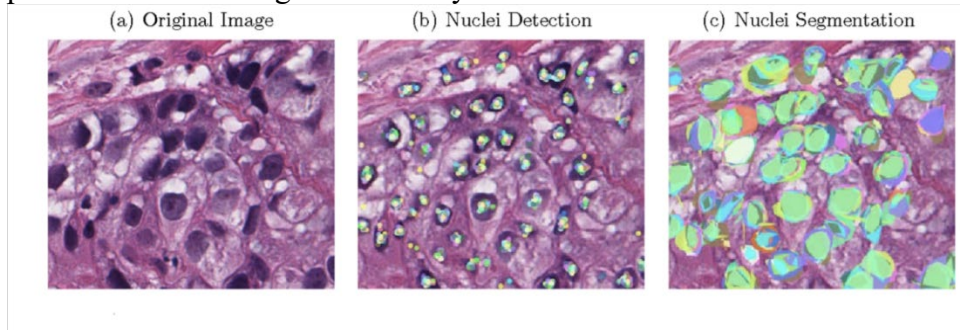

Fig. 1. Nuclei detection and segmentation process [3]

They have annotated their own dataset which they used for evaluation procedure, so there are no comparable results. In Chen et al. [10] design a deep contour-aware network. Their method and Tareef et al. [11] method achieves state-of-the-art results on their respective datasets. The difference between these and He et al. [12] is that Mask R- CNN does not focus on medical imaging and is not as heavily engineered. Mask R-CNN is a single model as well as easier to adapt and implement. However, it is the state-of-the-art for more general instance segmentation. In addition to it, it is more interesting to experiment with adapting a general instance segmentation model. It is especially conducted to solve the specific problem of instance segmentation of nuclei in medical imaging. The results from various methods are difficult to compare as they have not been evaluated on the same datasets. Table 1, summarizes the different state of the art techniques from the literature review of the current study.

According to the Literature review of the current study, the state of the arts are not focused on the overlapping of the cells, occluded nuclei. Moreover, limited attention

was given to the device independent solutions. The dataset used in this research was too resourceful, even having highly cluttered backgrounds and overlapping nuclei. The proposed methodology significantly improved the detection and segmentation accuracy.

III.Methodology

In this section, the researchers would represent the details on nuclei detection after using the modified UNet model, which is end-to-end fully convolutional network (FCN).

Table I
Summary of Literature Review Techniques

Paper	Method	Dataset	Result	Evaluation
Deep Learning Method Delineates Multiple Nuclear Phenotypes in H & E Stained Histology Section[8]	ENet	Private	0.6904	F-Score
ScanNet:A Fast & Dense Scanning Framework foe Metastatic Breast cancer Detection from Whole Side Images[5]	ScanNet	Camelyon16 [23]	0.8533	FROC
[ods.ai] topcoders Kaggle 2018 Data Science [13]	Unet	BBBC038v1 [4]	0.6316	Mean Average Precision
jacobkie Kaggle 2018 Data Science Bowl[[13]	UNetRCNN	BBBC038v1 [4]	0.6147	Mean Average Precision
Deep Retina Kaggle 2018 Data Science Bowl [13]	MRCNN	BBBC038v1 [4]	0.6140	Mean Average Precision

They first present the dataset and the architecture of the currently proposed Methodology. Thus, they discuss each phase of the proposed methodology.

A. Dataset

As discussed earlier, different datasets have been used for nuclei detection. In this research, they employed BBBC038v1 dataset for training and testing purpose.

Whereas, it was available from the Broad Bioimage Benchmark Collection and was the standard dataset for the Kaggle competition. All the images in the dataset had a height between 256 and 524 pixels and a width of between 161 and 696 pixels. The number of nuclei varied greatly; from only a couple to several hundred. The images had been captured under the different conditions. Furthermore, they varied in color, lighting, and the cells varied in types of cell. The dataset consisted of a training set of 670 images. On average there were $29461/670 = 44$ nuclei per training image. Eventually, there was a variety of background and foreground images in the dataset. There can be

1. Black foreground and white background
2. Purple background and (purple, white, yellow) foreground.
3. White foreground and black background

B. Proposed Method

The currently proposed methodology is based on U-Net. The height and width of the images are normalized to fed the proposed model. The proposed model is a modified version of U-Net. ELU activation function is used in their proposed solution. Where they employed BBBC038v1 dataset for conducting the training program and to fulfill the validation purpose. They also used 603 images as the training set and validation was performed on 67 images which was 10% of the total dataset. 65 images were used to evaluate the performance of our proposed solution. The basic architecture of the proposed methodology was given in Figure 2. The details of each step of the proposed solution was explained in the subsequent section.
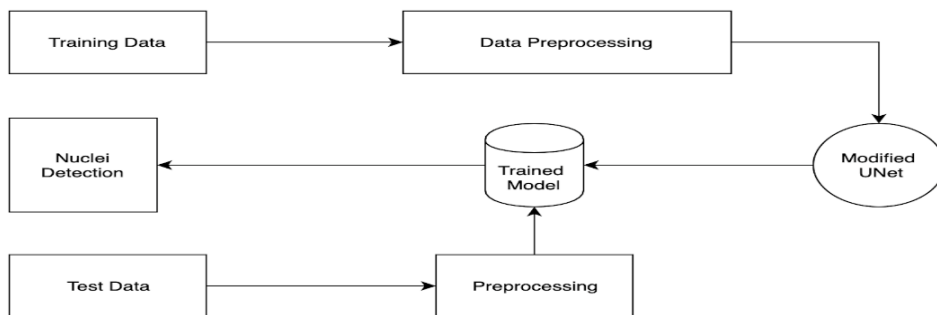

Fig. 2. Architectural diagram of proposed methodology

1. Data Preprocessing

In data pre-processing, data is modified or transformed into the useful format. Data can also exhibit many issues while data generation, therefore there is a need to pre-process it before using it. As explained earlier, the images in the dataset had the different height and width. In the pre-processing step, the size of all images is set to 256x256, so that we can pass them to the model for training. Suppose, the image I has the size $w \ x \ h$, and the resultant image is of size $w' \ x \ h'$, then for the each pixel in the input image, the new transformed coordinated would be

$$g(x',y') = I\left(\frac{w'x}{w}, \frac{h'y}{h}\right) \quad (1)$$

The resized images are then normalized

$$h(x',y') = \frac{g(x',y')}{max_{s,t} \, g(s,t)} \quad (2)$$

After the pre-processing of images, the images are fed to the proposed model for the nuclei detection.

2. Overview of U-Net Aechitecture

The currently proposed methodology is modified U-Net. U-Net is very popular for medical image segmentation. It is a fully convolutional network (FCN). There is a concept of skipping connection between different stages of U-Net, which gives superiority to its design [14].

The input-output mapping of linear networks can be represented

$$Out_n = W_{n-1}W_{n-2} \dots.. W_1 X \quad (3)$$

Where Out_n is the output and X is the input of the network. Moreover, W_j is the weight matrix between layer j and $j+1$ and j spans from 1 to $n-1$. For network with skip connections, this formulation is modified as

$$Out_n{}^{\Xi} = (W_{n-1} + I)(W_{n-2} + I) \dots.. (W_1 + I)X \quad (4)$$

Here $Out_n{}^{\Xi}$ is the output of skip connection network, having n layers. For non-linear networks, the input-output mapping can be formulated as

$$Out_n f(W_{n-1}f(W_{n-2}f(\dots.. f(W_1 X)))) \quad (5)$$

$$Out_n{}^{\Xi} = f((W_{n-1} + I)f((W_{n-2} + I)f(\dots.. f((W_1 + I)X)))) \quad (6)$$

f is the activation function. However, it applies some changes to deal with the trade-off between

localization and the use of context. This trade-off begins at the large patches, where there is a need of producing more pooling layers and reduce the accuracy of the localization. On the contrary, small patches can only perceive a small context of the information. There are two paths in U-Net model: analysis and synthesis. In the analysis path, U-Net follows CNN structure. The synthesis path is also called as the expansion phase. It contains an up-sampling layer and a deconvolution layer. Moreover, the important feature of U-Net is the shortcut connections between the layers. These connections exist between the layers which have an equal resolution. The deconvolution layers get high-resolution features from these connections. This architecture resembles the English alphabet 'U', therefore, it is called U-Net. U-Net is composed of the following three parts: The contraction section, the bottleneck section, and the expansion section. Furthermore, there are many contraction blocks in the contraction section. Each contraction block of this section takes an input and employs two convolution layers of size 3X3. After applying convolutions it applies a 2X2 max pooling. After each block, the number of the feature maps becomes double. Therefore,

architecture is the learning of too complicated structures. Hence, the last layer negotiates between the contraction layer and the expansion layer. In this layer, two 3X3 CNN layers are used and followed by 2X2 up convolution layer. Since, convolution is used without padding, the size of the output is less than the input size. Therefore, the strategy of overlapping is used instead of downsizing before network and up-sampling after the network. Thus, the image is predicted piece by piece in this technique.

3. Modified U-Net as Proposed Solution

Since unpadded convolution is used, the output size is smaller than the input size. Instead of downsizing before network and up-sampling after network, overlap tile strategy is used. Thereby, the whole image is predicted part by part.

In the original paper, the size of the input image is 572x572x3, however, they would use the input image of size 256x256x3. It largely decreases the feature size and computational cost. Hence, the size at various locations may differ from that in the original paper but the core components remain the same.

In this proposed solution, the researchers modified the U-Net

model to improve the accuracy of nuclei detection. For this purpose, they made some changes in Base U-Net architecture. The U-Net architecture uses RELU as the activation function. In the proposed solution, RELU is replaced with ELU [15]. Relu gives input in the range of 0 to a max value and it also gives the positive values against all the negative values. Converting all negative values directly into zero is a drawback and it is called "dying ReLU". In such a situation a ReLU neuron becomes "dead", it is stuck in case of the negative values and always gives 0 output. Because its slope in case of a negative range is also 0. ReLU cannot recover a neuron once its value becomes 0, the neuron becomes useless and it cannot play any role in distinguishing the input. In the result, a large portion of the network would not take any part in the training.

Anyhow, the activation function named as an Exponential Linear Unit or its widely known name ELU was used. Researchers revealed that the function converges cost to zero faster and gives very accurate results. Therefore, ELU was adopted in our proposed solution to improve the performance of the model. Mathematically ELU is defined as

$$f_{ELU}(x) = \begin{cases} e^x - 1 & ; for\ x < 0 \\ x; & for\ x \geqslant 0 \end{cases}$$

(7)

For back propagation, the derivative of positive values will be one and for negative values that derivative will be e^x. These properties lead to faster training and better accuracies. Also, it does not suffer from dying neuron problem or exploding/vanishing gradients.

Moreover, the researchers introduce a drop-out layer between two convolutional layers of every block to avoid overfitting. Large neural network trained on relatively small datasets can over fit the training data. This has led to the effects of the model learning focusing on the statistical noise in the training data. Furthermore, it results into the poor performance when the model is evaluated on new data, that is, a test dataset. Hence, the generalization decreases due to the overfitting process as the generalization error increases. The architecture of proposed methodology (modified U-Net) is shown in Figure 3. As the output Softmax function is applied on each pixel of the resultant image to achieve multi-class segmentation problem. Cross-entropy function is used for loss calculation and updating weights. Softmax function and cross entropy is defined as

$$\sigma(\vec{z})_i = \frac{e^{z_i}}{\sum_{j=1}^{k} e^{z_j}} \qquad (8)$$

$$Loss_{CE} = -\sum_i^C t_i \log(\sigma(\vec{z})_i) \quad (9)$$

Where $\vec{z}$ is an input vector and σ is the softmax output.

We used Adam optimizer with the learning rate to 0.001 for training. Adam optimizer is used to accelerate the gradient descent algorithm. It includes exponentially weighted average of the gradients,

resulting in faster convergence. Mathematically,

$$w_{t+1} = w_t - \propto \xi_t \qquad (10)$$

$$\xi_t = \beta \xi_{t-1} + (1-\beta)\left[\frac{\delta Loss_{CE}}{\delta w_t}\right]$$
$$(11)$$

Where,

$\xi_t = aggregate\ of\ gradient\ at\ time\ t$

$\propto = learning\ rate$

$\beta = Moving\ average\ parameter$
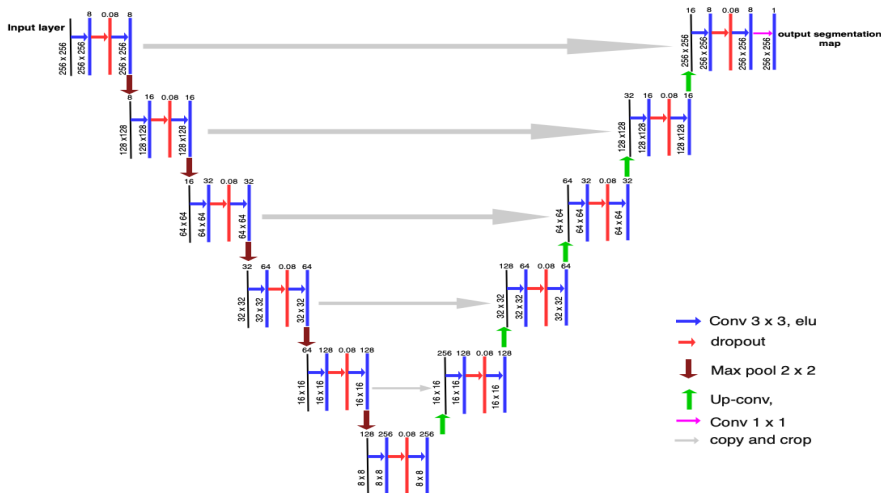
Fig. 3. Modified U-Net architecture.

IV. Results & Discussion

This section presents the details of the experiments which were carried out to evaluate our proposed methodology. The researchers conducted different experiments for the evaluation of proposed solution. They used Google Colab with 12GB memory and 48 GB Disk space to perform our experiments. They employed BBBC038v1 dataset and computed very promising results.

The details of dataset division and computed results are explained in subsequent section.

The dataset contains 735 images in total, we used 603 images for training and 67 images for validation purpose. They used the above mentioned experimental settings and performed three different experiments. IOU is the evaluation metrics, which is mostly employed in object detection problem to measure the accuracy of model. The IOU is computed between the ground truth bounding box of original images and predicted bounding box. The IOU between predicted pixels (A) of model and ground truth pixels (B) can be computed as

$$IOU(P,Q) = \frac{P \cap Q}{P \cup Q} \qquad (12)$$

IOU is the most commonly used metric for object detection and segmentation. IOU is a vital metric to track the tasks of human annotation. Therefore, it is widely used in medical imaging problems. Other evaluation metrics like MAP (Mean Average Precision) does not show that how closely it has been predicted the output and how far it matches with the actual outcome.

IOUs tell precisely that how much the prediction matches/deviates from the ground truth.

They also used ELU as the activation function. Moreover, a dropout has also been introduced between the every two convolutional layers so that we can avoid overfitting.

The model is trained on different epochs where we realized that at 19th epoch, the training loss is minimum and value of IOU is maximum. Therefore, we stopped the training process and saved the model. The training and validation loss of the model is shown in Fig. 4. Also, the training and validation accuracy of the model is shown in Fig 5.

In order to evaluate the trained model, the researchers used 65 images as a test set, where they fed the test images to model and model computed IOU between ground truth information of original image and predicted labels. They also computed 0.78 IOU value over the test set which is greater than the previously reported results. The sample image of nuclei detection is shown in Fig. 6.
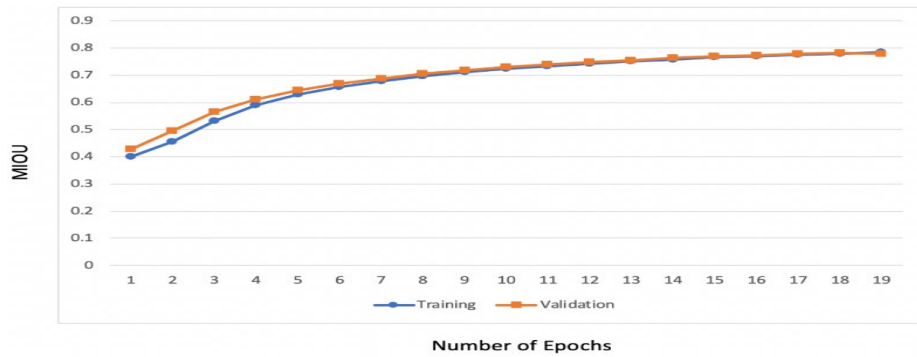
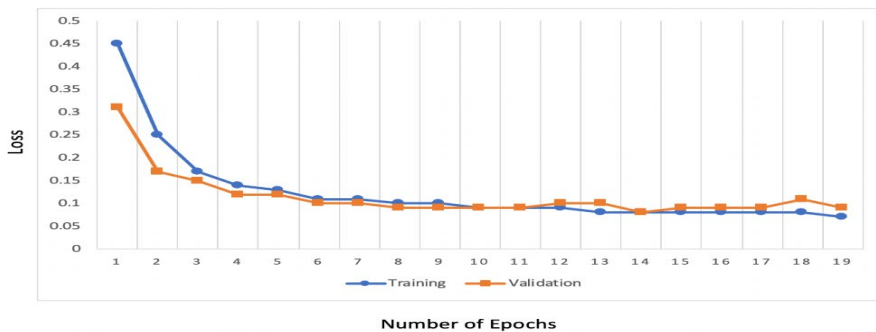**Fig. 4.** Training and validation accuracy of proposed methodology.

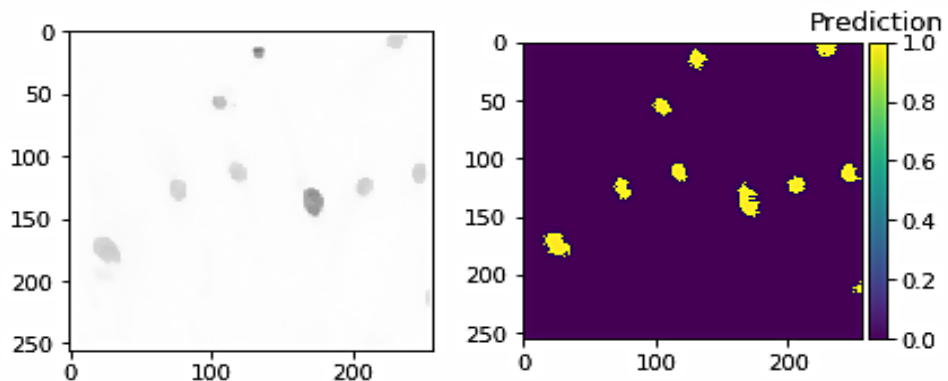**Fig. 5.** Training and validation loss of proposed methodology.

Fig. 6. Pictorial representation of nuclei detection.

Moreover, for the verification of our proposed solution we performed some more experiments. In the second experiment RELU is used as the activation function. They did not normalize the input and no

dropout is used in this presented setup. The model is trained on different epochs. They computed 0.63 IOU value over test set. The training and validation loss of the model is shown in Fig. 7. Also, the training and validation accuracy of the model is shown in Fig.
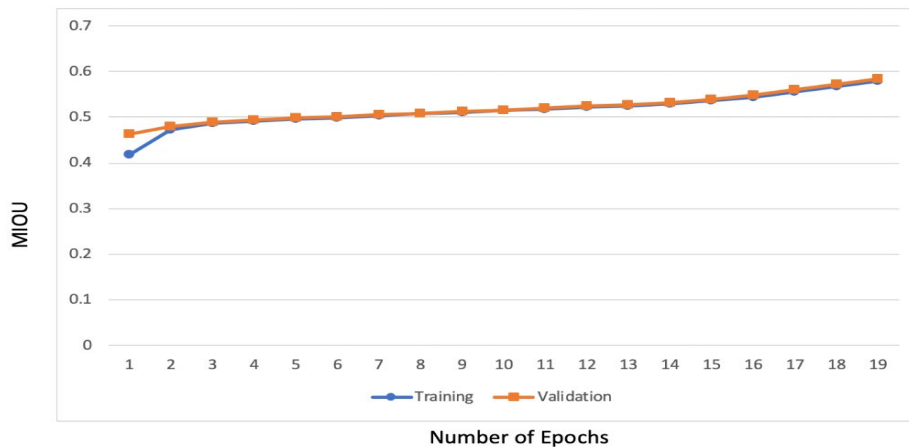

Fig. 7. Training and validation accuracy using RELU activation function without dropout layer.
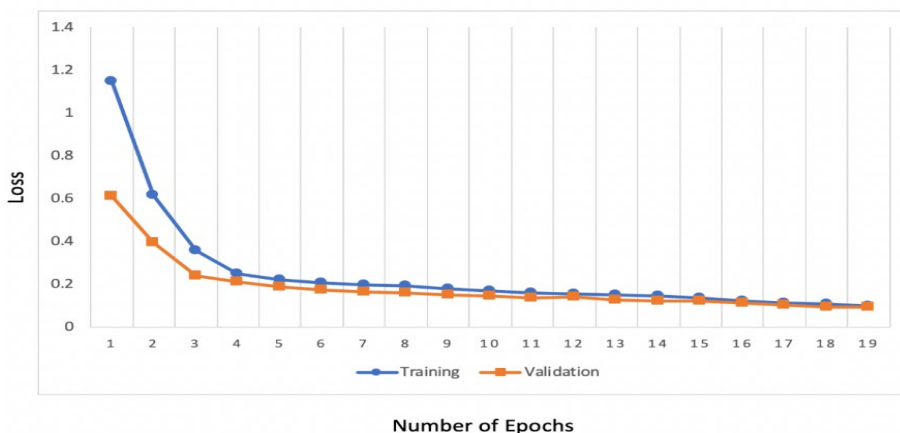

Fig. 8. Training and validation loss using RELU activation function without dropout layer.

In the third experiment we used RELU as the activation function. They performed the experiment with dropout layer. The model is trained on different epochs. They computed 0.58 IOU value over the

test set. The training and validation loss of the model is shown in Fig. 9. Also, the training and validation accuracy of the model is shown in Fig. 10.
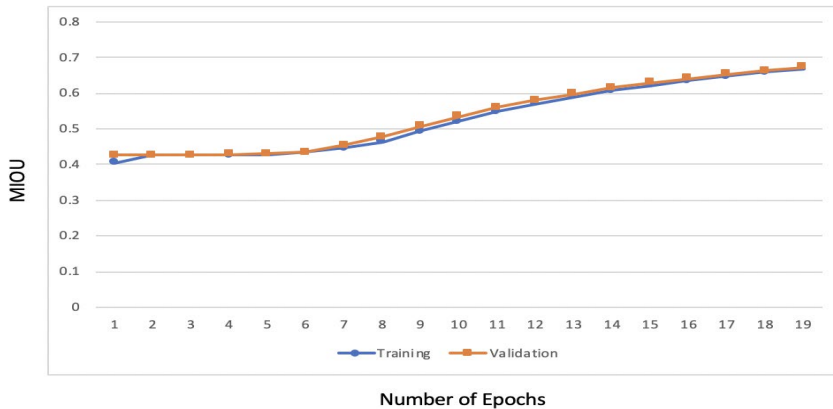

Fig. 9. Training and validation accuracy using RELU as activation function with dropout layer.
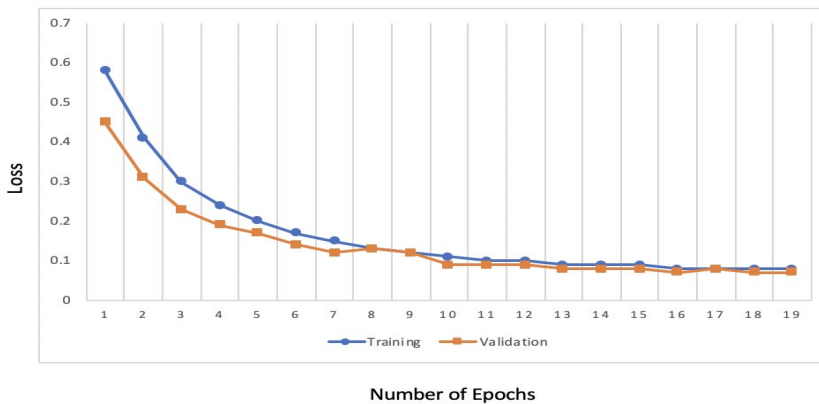

Fig. 10. Training and validation loss using RELU as activation function with dropout layer.

In the fourth experiment we used RELU as the activation function. They performed the experiment with dropout layer and with normalization of data. The model is trained on different epochs. They computed 0.67 IOU value over the test set. The training and

validation loss of the model is shown in Fig. 11. Also, the training and validation accuracy of the model is shown in Fig. 12. Hence, it is clear from the above-conducted experiments, that our proposed solution gives better results with 0.78 IOU value.
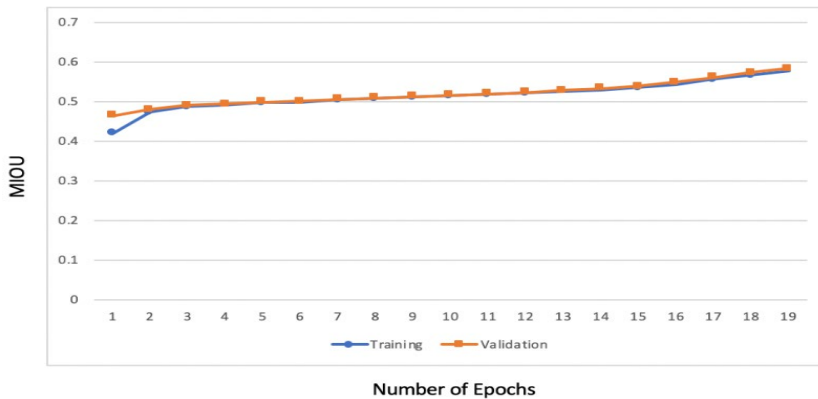

Fig. 11. Training and validation accuracy using RELU as activation function with dropout layer and lambda function.
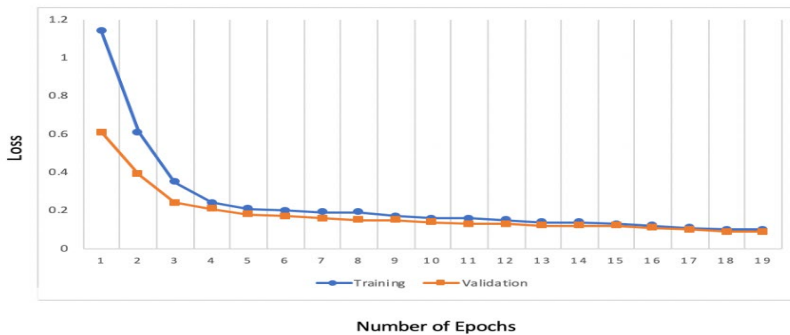

Fig. 12. Training and validation Loss using RELU as activation function with dropout layer and lambda function.

As the researchers are inspired from Kaggle Nuclei Detection Competition, so they are going to compare the proposed solution results with the top scorer of that competition. Table 2 shows the comparison of the proposed scheme with state of the art. Below is given the comparison of that Table which shows the proposed methodology which improved the accuracy of nuclei detection.

Table II
Comparison of Results of Proposed Methodology

Paper	Method	Dataset	Result	Evaluation
Deep Learning Method Delineates Multiple Nuclear Phenotypes in H & E Stained Histology Section [5]	ENet	Private	0.6904	F-Score
Scan Net: A Fast & Dense Scanning Framework foe Metastatic Breast cancer Detection from Whole Side Images [18]	ScanNet	Camelyon16 [16]	0.8533	FROC
[ods.ai] Top coders Kaggle 2018 Data Science [13]	UNet	BBBC038v1	0.6316	Mean Average Precision
Jacobkie Kaggle 2018 Data Science Bowl[[13]	UNetRCNN	BBBC038v1	0.6147	Mean Average Precision
Deep Retina Kaggle 2018 Data Science Bowl [13]	MRCNN	BBBC038v1	0.6140	Mean Average Precision
Proposed Methodology	Modified UNet	BBBC038v1	0.78	Mean Average Precision

V. Conclusion

The current study focused on the detection and the localization of nuclei in medical images by using a modified and advanced U-Net model. In this study, researchers employed the modified version of U-NET in order to detect the nuclei in medical images. Whereas, publicly available standard benchmark BBBC038V1 is used for model training and testing in this research. Dataset contains strenuous images with overlapping nuclei, cluttered backgrounds, varying lightening conditions and variety of acquisition devices, and configurations. The proposed research works well on these challenging test cases. The researchers performed different experiments for the evaluation of the proposed solutions. They also observed the presented model

improved accuracy (IOU value) 24% better than the non-modified model. IOU score of 0.78 over test set is reported by the presented research. From now on, the combination of different models can be used to improve the detection of nuclei. Moreover, U-Net model can also be modified to increase the detection and localization rate, that is, Ladder-Net, which also can be used for such complex detection tasks. Hence, the different advanced techniques can be used to solve this complex detection problem.

References

[1] M. Z. Alom, C. Yakopcic, T. M. Taha, and V. K. Asari, "Microscopic nuclei classification, segmentation and detection with improved deep convolutional neural network (dcnn) approaches," *arXiv preprint*, arXiv e1811.03447, 2018, doi:

https://doi.org/10.48550/arXiv.1811.03447

[2] M. G. Rojo, V. Punys, J. Slodkowska, T. Schrader, C. Daniel, and B. Blobel, "Digital pathology in Europe: Coordinating patient care and research efforts," *Stud. Health Technol. Inform.*, vol. 150, pp. 997–1001, 2009, doi:

https://doi.org/10.3233/978-1-60750-044-5-997

[3] H. Irshad et al., "Crowdsourcing image annotation for nucleus detection and segmentation in computational pathology: evaluating experts, automated methods, and the crowd," in *Pac. Sympos. Biocomput.,* 2014, pp. 294-305. https://doi.org/10.1142/9789814644730_0029

[4] Broad BioImages Benchmark Collection, "Kaggle 2018 data science bowl, 2019," Broad BioImages Benchmark collection.

[5] T.-Y. Lin, P. Goyal, R. Girshick, K. He, and P. Dollár, "Focal loss for dense object detection," in *Proc. IEEE Int. Conf. Comput. Vision.*, 2017, pages 2980–2988.

[6] D. Bhattacharjee and A. Paul, "A leukocyte detection technique in blood smear images using plant growth simulation algorithm," in *31st AAAI Conf. Artifi. Inteell.*, 2017.

[7] T.-Y. Lin, P. Goyal, R. Girshick, K. He, and P. Dollár, "Focal loss for dense object detection," in *Proc. IEEE Int. Conf. Comput. Vision.*, 2017, pages 2980–2988.

[8] M. Khoshdeli and B. Parvin, "Feature-Based representation improves color decomposition

and nuclear detection using a convolutional neural network," in *IEEE Transac. Biomed. Eng.*, vol. 65, no. 3, pp. 625-634, Mar. 2018, doi: https://doi.org/10.1109/TBME.2017.2711529

[9] Y. Xie, F. Xing, X. Shi, X. Kong, H. Su, and L. Yang, "Efficient and robust cell detection: A structured regression approach," *Med. Image Anal.*, vol. 44, pp. 245–254, 2018, doi: https://doi.org/10.1016/j.media.2017.07.003

[10] H. Chen, X. Qi, L. Yu, Q. Dou, J. Qin, and P.-A. Heng. *Dcan: Deep contour-aware networks for object instance segmentation from histology images*. Medical Image Analysis, 36:135–146, Feb. 2017, doi: https://doi.org/10.1016/j.media.2016.11.004

[11] A. Tareef, Y. Song, H. Huang, Y. Wang, D. Feng, M. Chen, and W. Cai, "Optimizing the cervix cytological examination based on deep learning and dynamic shape modeling," *Neurocomputing*, vol. 248, pp. 28–40, 2017, doi: https://doi.org/10.1016/j.neucom.2017.01.093

[12] K. He, G. Gkioxari, P. Dollár, and R. Girshick, "Mask R-CNN.

(2018)," arXiv. arXiv preprint arXiv:1703.06870.

[13] Kaggle Combination, "Kaggle 2018 data science bowl competition," Broad BioImages Benchmark collection.

[14] Kaggle Combination, "Kaggle 2018 data science bowl competition, 2018," Broad BioImages Benchmark collection. https://www.kaggle.com/competitions/data-science-bowl-2018

[15] Broad Institute, "Kaggle 2018 data science bowl, 2019," Broad BioImages Benchmark collection. https://bbbc.broadinstitute.org/BBBC038

[16] O. Ronneberger, P. Fischer, and T. Brox, "U-net: Convolutional networks for biomedical image segmentation," in *Int. Conf. Med. Image Comput. Computer-Assisted Interv.*, Navab, N., Hornegger, J., Wells, W., and Frangi, A. Eds., Cham, Springer, 2015, pp. 234–241, doi:https://doi.org/10.1007/978-3-319-24574-4_28

[17] D.-A. Clevert, T. Unterthiner, and S. Hochreiter, "Fast and accurate deep network learning by exponential linear units (elus)," *arXiv preprint*,

arXiv:e1511.07289, 2015, doi: https://doi.org/10.48550/arXiv.1511.07289

[18] ISBI, "ISBI challenge on cancer metastasis detection in lymph node," ISBI. https://camelyon16.grand-challenge.org/Results/ (accessed Feb. 9, 2022).